Wireless Pers Commun (2016) 88:223–239
DOI 10.1007/s11277-015-3089-4

A Low Complexity Peak-to-Average Power Ratio Reduction Scheme Using Gray Codes

Mohsen Kazemian[1] · Pooria Varahram[1] · Shaiful Jahari Bin Hashim[1] · Borhanuddin Mohd Ali[1] · Ronan Farrell[2]

Published online: 13 October 2015

Abstract A low-complexity peak-to-average power ratio (PAPR) reduction scheme in an orthogonal frequency division multiplexing system is proposed. The proposed scheme utilizes a new phase sequence based on a gray code structure and a similarity measurement block. Due to the ordered phase sequences, a noteworthy reduction capacity is obtained in terms of the number of multiplication and addition operations and the side information. Simulations are performed with quadrature phase shift keying modulation and a Saleh model power amplifier. The proposed scheme offers a significant PAPR reduction and bit error rate performance at approximately the same total complexity compared to the conventional partial transmit sequence and the enhanced partial transmit sequence (EPTS) techniques. The results show that at the same PAPR reduction, this scheme provides a complexity reduction of at least 42.3 % over that of the EPTS technique.

Keywords BER · OFDM · PAPR · PTS · Gray code

✉ Mohsen Kazemian
mohsen_kazemian@yahoo.com; mohsen.kazemian.my@ieee.org

Pooria Varahram
varahram@upm.edu.my

Shaiful Jahari Bin Hashim
sjh@upm.edu.my

Borhanuddin Mohd Ali
borhan@upm.edu.my

Ronan Farrell
rfarrell@eeng.nuim.ie

[1] Department of Computer and Communications System Engineering, Universiti Putra Malaysia, 43400 UPM Serdang, Selangor, Malaysia

[2] Institute of Microelectronics and Wireless Systems, National University of Ireland, Maynooth, Ireland

1 Introduction

A new generation of wireless communication systems should be able to provide some major specifications, such as the ability to transmit at a high data rate with emphatic constraints on the power consumption and bandwidth seizure. Hence, it is necessary to adopt the Power-efficient and M-ary modulation schemes with a high spectral efficiency, including quadrature amplitude modulation (4-QAM) in conjunction with orthogonal frequency-division multiplexing (OFDM). Because of the OFDM benefits, the use of this technique for cellular mobile radio standards, LTE and future wireless standards is prevalent. When considering several research reports, a major drawback of the OFDM signals is a high peak-to-average power ratio (PAPR) [1] because a large PAPR leads to in-band distortion, out-of-band radiation and efficiency degradation [2, 3].

To date, several PAPR-reduction techniques to mitigate these problems have been proposed in the literature, including probabilistic techniques [4, 5], coding [6, 7], companding [8, 9], selected mapping (SLM) [10], partial transmit sequence (PTS) [11–15], tone reservation (TR) [16], active constellation extension (ACE) [17], cross-correlation-PTS [18], and clipping and filtering (CAF) [19, 20]. It should be mentioned that clipping is the simplest method, but it causes BER degradation and interference in the adjacent channels.

One specific approach that has received much attention is the PTS technique. However, one of its major drawbacks is its high computational complexity [21, 22]. The conventional PTS (CPTS) technique is based on different phase sequences and ultimately selects the optimum phase sequence from the sequences that can produce the minimum PAPR. The optimization has been carried out either by using efficient search processes to select the optimum phase sequence [21] or by using several optimization metrics, such as the intermodulation distortion (IMD) [23], the peak interference-to-carrier ratio (PICR) [24], the mean squared error (MSE) [25] and the distortion-to-signal power ratio (DSR) [26]. The use of these metrics would have a high impact on the system's bit error rate (BER) [23, 26].

Al-Dalakta [18], proposed a new method called the cross-correlation PTS, which has a low complexity, for reducing the BER. The CPTS technique is more efficient in terms of the PAPR reduction compared to the cross-correlation PTS, which means that the cross-correlation PTS technique is not able to improve the PAPR as well as the CPTS technique can.

Varahram [13], proposed a new phase sequence, which has an advantage for the number of inverse fast Fourier transforms (IFFTs), but some drawbacks, such as a high number of multipliers in each iteration, an inability to support high iterations, the need to save a large side information matrix as well as useless iterations due to the random phase sequences, are significant.

This paper presents a new low-complexity technique to reduce the PAPR capacity and the BER degradation of the OFDM systems due to the non-linear characteristics of the high power amplifier (HPA). The structure of the proposed method is different from the CPTS technique because of the use of two blocks for sorting the effects of the different phase sequences on the PAPR and for the similarity measurements. Therefore, by using a new phase sequence based on the Gray code and one similarity measurement block, a technique with a smaller number of IFFTs and multipliers, can be achieved with acceptable BER and PAPR reduction results.

This paper is organized as follows. Section 2 summarizes the PAPR and the power amplifier. In Sect. 3, the PTS technique and the proposed scheme are introduced. Sections 4 and 5 present the simulation results and the conclusion, respectively.

2 PAPR Definition and Power Amplifier Model

A multicarrier signal is the sum of many independent signals that are modulated onto sub channels of equal bandwidth. The complex baseband representation of a multicarrier signal consisting of N subcarriers is given by

$$x(t) = \frac{1}{\sqrt{N}} \sum_{k=0}^{N-1} X_{(k)} e^{j2\pi k \Delta f t} \quad 0 \le t < NT \tag{1}$$

where $j = \sqrt{-1}, X_{(k)}$ is the data symbol of the kth subcarrier, N is the number of subcarriers, Δf is the subcarrier spacing, and T is the OFDM symbol duration $\left(\Delta f = {}^{1}/_{NT}\right)$. The PAPR is a measure that is generally used to quantify the envelope variations of the multicarrier signals and can be defined as [20]:

$$PAPR = \frac{\max_{0 \le t \le T} \left[|x(t)|^2 \right]}{E\left[|x(t)|^2 \right]} \tag{2}$$

where $E[\cdot]$ denotes an expectation. The most popular metric for measuring the PAPR is the complementary cumulative distribution function (CCDF) [27, 28]. The CCDF of the PAPR denotes the probability that the PAPR of a data block exceeds a given threshold, and it is defined as follows:

$$CCDF = \Pr(PAPR > PAPR_0) \tag{3}$$

where $PAPR_0$ is the given threshold. The CCDFs are mostly compared in a graph for which the horizontal and vertical axes demonstrate the threshold and the probability that the PAPR exceeds the threshold, respectively.

In this paper, the memory-less nonlinear power amplifier Saleh model is used to describe the effects of the PAPR for HPA efficiency.

The *AM/AM* and *AM/PM* characteristics of the Saleh model amplifier can be expressed as [13, 30]:

$$\phi(t) = \frac{\pi}{6} \frac{x(t)}{x(t)^2 + Z_{sat}^2} \tag{4}$$

$$Y(t) = Z_{sat}^2 \frac{x(t)}{x(t)^2 + Z_{sat}^2} \tag{5}$$

where $x(t)$ is the absolute value of the input signal, Z_{sat} indicates the amplifier input saturation voltage behavior, and finally, $\phi(t)$ and $Y(t)$ are the *AM/PM* and *AM/AM* of the power amplifier, respectively. It should be mentioned that 2.5 is the value which used as the gain of this amplifier.

3 Proposed Method

3.1 Conventional Partial Transmit Sequence (CPTS)

The PTS technique's structure is defined by dividing an input signal X of N symbols into V disjoint subblocks

$$X_V = \left[X_{v,0}, X_{v,1}, \ldots, X_{v,N-1}\right]^T \quad v = 1, 2, \ldots, V \tag{6}$$

where $\sum_{v=1}^{V} X_v = X$. The subcarriers in these subblocks are multiplied by the phase sequences in the time domain and are introduced as $b_v = e^{j\phi_v}, v = 1, 2, \ldots, V$. The set of phase factors is denoted as a vector $b = [b_1, b_2, \ldots, b_V]^T$. The time domain signal after this combination is given by

$$X^{'}(b) = \sum_{v=1}^{V} b_v . X_v \tag{7}$$

where $X^{'}(b) = [x_0'(b), x_1'(b), \ldots, x_{NL-1}'(b)]^T$ and L is the over-sampling factor [28, 29]. Let us interpret the collection of all data symbols X_k, $k = 0, 1, \ldots, NL-1$ as a vector $X = [X_0, X_1, \ldots, X_{NL-1}]^T$. The selection of the optimum phase sequence is dependent on the minimization of the PAPR for the combined signal, and minimization of the PAPR is related to the minimization of $\max_{0 \le k \le NL-1} \left|x_k^{'}(b)\right|$.

Enhanced partial transmit sequence (EPTS) technique [13] can perform a similar PAPR reduction by using half the number of IFFT blocks compared to the CPTS technique. This phase sequence is defined as

$$B = \begin{bmatrix} b1,1 & ,\ldots, & b1,N \\ \vdots & \vdots & \vdots \\ bv,1 & \ldots & bv,N \\ bv+1,1 & ,\ldots, & bv+1,N \\ \vdots & \vdots & \vdots \\ b_P,1 & ,\ldots, & b_P,N \end{bmatrix}_{P \times N} \quad v = 1, 2, \ldots, V \tag{8}$$

where P is the number of iterations, which can be calculated as follows:

$$P = DW^{V-1} \quad D = 1, 2, \ldots, D_N \tag{9}$$

where D is the coefficient that specifies the PAPR reduction capacity and D_N is determined by the user, V is the number of subblocks and W is the number of allowed phase factors.

For $N = 256$, 256 multipliers are needed for each row, and therefore a huge number of multipliers are needed by increasing the number of rows. Hence, in EPTS technique [13], the iteration number is P, while for the CPTS scheme; the W^{V-1} iteration is needed to find the optimum phase sequence.

3.2 The Proposed Gray Code-Based Phase Sequence

In this paper, a new phase sequence is proposed to decrease the total complexity in each iteration. *Hence, the proposed method enables more iterations to be made by using a less multiplier numbers compared to the CPTS and EPTS techniques*. This new phase sequence

is based on the Gray code. The Gray code is a code pattern whose adjacent code strings differ for only one bit [31]. One type of Gray code is the n-ary Gray code. A 4-ary Gray code would use the values {0, 1, 2, 3}. The sequence of elements in the 4-Gray code can be explained using the following matrices. If

$$e = \begin{bmatrix} 0 \\ \vdots \\ 0 \end{bmatrix}_{l\times 1} \quad f = \begin{bmatrix} 1 \\ \vdots \\ 1 \end{bmatrix}_{l\times 1} \quad g = \begin{bmatrix} 2 \\ \vdots \\ 2 \end{bmatrix}_{l\times 1} \quad h = \begin{bmatrix} 3 \\ \vdots \\ 3 \end{bmatrix}_{l\times 1} \quad \text{and} \quad Q = \begin{bmatrix} e \\ f \\ g \\ h \end{bmatrix}_{(4\times l)\times 1},$$
$$\tilde{Q} = \begin{bmatrix} h \\ g \\ f \\ e \end{bmatrix}_{(4\times l)\times 1} \tag{10}$$

Then, the 4-ary Gray code can be explained as follows:

$$M = \begin{bmatrix} [Q(l=64)]_{256\times 1} & \begin{bmatrix} Q(l=16) \\ \tilde{Q}(l=16) \\ Q(l=16) \\ \tilde{Q}(l=16) \end{bmatrix}_{256\times 1} & \begin{bmatrix} Q(l=4) \\ \tilde{Q}(l=4) \\ Q(l=4) \\ \vdots \\ \tilde{Q}(l=4) \\ Q(l=4) \\ \tilde{Q}(l=4) \end{bmatrix}_{256\times 1} & \begin{bmatrix} Q(l=1) \\ \tilde{Q}(l=1) \\ Q(l=1) \\ \vdots \\ \tilde{Q}(l=1) \\ Q(l=1) \\ \tilde{Q}(l=1) \end{bmatrix}_{256\times 1} \end{bmatrix}_{256\times 4} \tag{11}$$

where l is the number of rows that is different in the above matrices, and $Q(l = L)$ and $\tilde{Q}(l = L)$describe the Q and $\tilde{Q}$ matrices, which are made using the *e, f, g, h* matrices by l rows.

The 4-ary Gray code is a sequence of bit strings, which can be formatted as a 256 × 4 matrix. *{0,0,0,0}, {0,0,0,1}, {0,0,0,2}, {0,0,0,3}* are the starting fourth codes, and *{3,0,0,3}, {3,0,0,2}, {3,0,0,1}, {3,0,0,0}* are the last fourth codes that are shown here as examples for better perception. The matrix M extends to $\tilde{M}$ as a newly defined matrix:

$$\tilde{M} = \begin{bmatrix} \overbrace{M \quad , \ldots , \quad M}^{N/4} \end{bmatrix}_{256\times N} \tag{12}$$

where N is the number of subcarriers. This is a new phase sequence called the Gray code-based phase sequence (GCP).

Refer to (8), matrix B has P rows and N columns of a random phase sequence. If $P = 256$ and $N = 256$, 256 × 256 multipliers are needed. This is a huge number of multipliers. In addition, because of the random phase sequences at each row, a significant change is not guaranteed after each iteration compared to the previous iteration. Moreover, if a smaller number is selected as the P parameter, the efficiency and PAPR reduction terms cannot satisfy the requirements.

In the proposed phase sequence with the Gray code, only *N/4* multipliers are needed in each row, which means 1 phase difference for each of the 4 phases. So for $P = 256$ and

$N = 256$, 256×64 multipliers are needed. Matrix $\tilde{M}$ has 4 phases for $N/4$ times and is introduced as $\{b_0, b_1, b_2, b_3\}$. The first line can be calculated as follows:

$$Y_1 = \left\{ \underbrace{b_{1,0}x_{(0+4n)}}_{N/4}, \underbrace{b_{1,1}\, x_{(1+4n)}}_{N/4} \underbrace{b_{1,2}x_{(2+4n)}}_{N/4} \underbrace{b_{1,3}x_{(3+4n)}}_{N/4} \right\}_{0 \le n \le N/4-1} \tag{13}$$

where $x_{(.)}$ denotes the input symbol number.

The calculation of the same x at the next iteration is related to the next phase sequence. Figure 1 illustrates the phase multiplication procedure. If $Y_1 = \{y_0, y_1, y_2, y_3\}$, and the next phase sequence has one bit difference at the second bit and is defined as $\{b_0, b_1^{'}, b_2, b_3\}$, it can easily be achieved as $\{y_0, y_1^{'}, y_2, y_3\}$ where the calculation of $y_1^{'}$ is the same as y_1 when $b_1^{'}$ is the considered phase instead of b_1. Thus, all the iteration results can be obtained according to the previous iteration. Vector z, which is specified in Fig. 2 for the kth iteration using the jth phase number, is defined as

$$z_{k,j} = \underbrace{\sum_{i=1}^{V} b_{j,k-1+i}\, x_{i,(j+4n)}}_{N/4} \quad 0 \le n \le N/4 - 1 \tag{14}$$

Vector $z_{k,j}$ has $N/4$ elements. The extension of the above vector for all 4 phases can be defined as:

$$z_k = \left\{ z_{k,j} \right\}_{j=0,1,2,3} \tag{15}$$

The next iteration vector can be calculated by the previous vector:

$$z_{k+1} = \left\{ z_{k,j_{j \neq j'}}, y_{j'} \right\} \tag{16}$$

where j' is the bit number of the$(K + 1)$th iteration, which differs from the previous iteration.

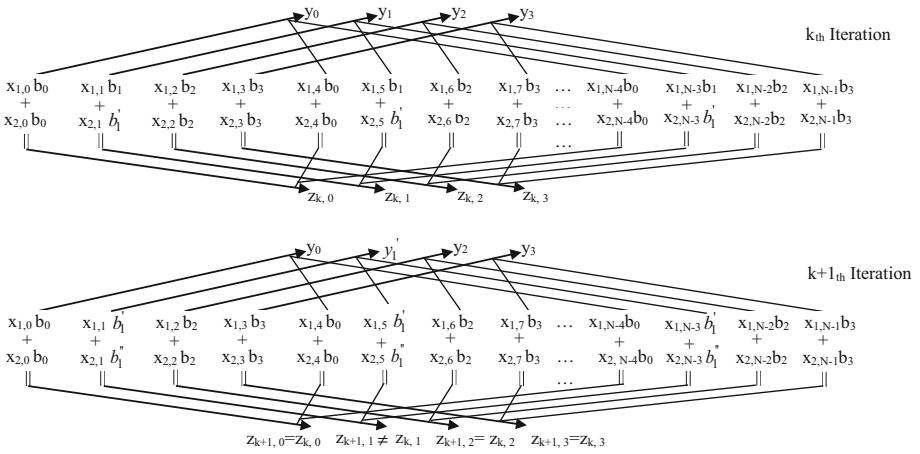

Fig. 1 Proposed phase sequence and the multiplication procedure by V = 2

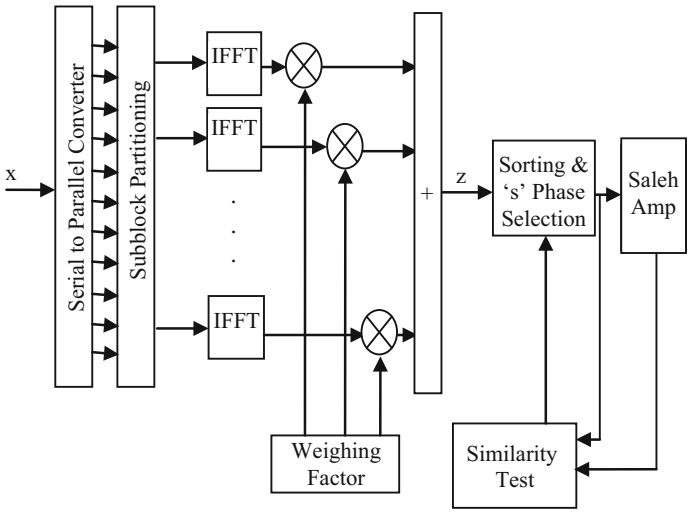

Fig. 2 Block diagram of the proposed PTS method

As mentioned above, a 4-bit Gray code string differs by only one bit from the previous or the next string and needs one multiplier for each string change. Therefore, a 4-ary Gray code, which has 256 strings, needs 256 multipliers, as shown in (11).

The other complexity reduction issue is the special phase sequences allocation called the enhanced Gray code-based phase sequence (EGCP). Consider the number of allowed phase factors $W = 4$ so that the phase sequence can be chosen from *{1, j, −1, −j}*. As mentioned above, an M-ary Gray code uses the values *{0, 1, 2, 3}*. The main concept is the assignment of the *'0'* code to *'1'*, the *'1'* code to *'−1'*, the *'2'* code to *'-j'*, and the *'3'* code to *'j'*. By this phase sorting, only for passing the code *'1'* to *'2'* and *'3'* to *'0'*, one multiplier is needed, and the other changes would only be produced by one sign change: '+' to '−' or '−' to '+'. For example, changing the code *{1, 2, 0, 0}* to *{1, 1, 0, 0}* is equal to changing the phase sequence *{−1, −j, 1, 1}* to *{−1, −1, 1, 1}*. Clearly, the second phase has been changed and needs one multiplier. Changing the code *{1, 1, 0, 0}* to *{1, 1, 0, 1}* is equivalent to changing the phase sequence *{−1, −1, 1, 1}* to *{−1, −1, 1, −1}*. The change in the last phase is achieved by one sign change and does not require a multiplier. It should be noted that this matrix sorting does not result in a complicated proposed procedure because the position of the multipliers and the sign-changing positions are exactly assigned.

For a *4-ary Gray code* with *256* rows in the above analysis, the necessary multiplier positions are defined as follows:

$$\beta = 4\alpha + 2 \quad \alpha = 0, 1, \ldots, 63 \tag{17}$$

$$\beta' = 16\alpha' + 8 \quad \alpha' = 0, 1, \ldots, 15 \tag{18}$$

$$\beta'' = 64\alpha'' + 32 \quad \alpha'' = 0, 1, 2, 3 \tag{19}$$

where β, β' and β'' are the positions that need multipliers.

Hence, the 256 multipliers in matrix M are replaced by only 85 multipliers and finally the used matrix is decreased from 256×256 multipliers in (8) to 85×64 multipliers and

becomes an optimum phase sequence matrix with low complexity and better PAPR reduction because more iterations are used. Additionally, because of the use of fixed phase sequences rather than random phase sequences, the results are guaranteed.

3.3 Proposed Structure

The proposed structure method is shown in Fig. 2. According to (6) and (7), the new vector G_i can be defined as

$$G_i = \max\left|X^{'}(b)\right| \quad 1 \le i \le P,\ 1 \le P \le 256 \tag{20}$$

where $G_i = [x_1^{''}, \ldots, x_P^{''}]$ and P is the number of iterations, which is flexible and is specified by the user. After saving the vector $G_i$and one ascending sorting stage, the new vector R is obtained as

$$R = [r_1, \ldots, r_S, \ldots, r_P],\ 1 \le S \le P,\ r_1 \le r_2 \le \ldots \le r_P \tag{21}$$

As mentioned above, P is the iteration number that is equal to the length of vector R, and S is the selected number of R elements.

Note that the R vector elements are similar to the G_i vector elements, but on an ascending mode.

The effect of the power amplifier on a signal can be approximated using one amplifier model. If the power amplifier operates at a linear region or the maximum signal level is below the amplifier saturation point, the input and output of the amplifier shape are equal [18, 30]. Therefore, the similarity measurement method can be used to figure out the degree of the amplifier input and the output similarity.

In statistics, the cross-correlation (CCOR) and the Sorensen–Dice coefficient (SDC) are two similarity test methods between two variables, x and y. The CCOR can be defined as

$$R_{xy}^{(0)} = \sum_{n=0}^{N-1} x_n y_n^* \tag{22}$$

Additionally, the SDC is expressed as

$$SDC = \frac{2|x.y|}{|x|^2 + |y|^2} \tag{23}$$

So, the S members from vector Z, which are specified by the user should pass through an amplifier, where x and y are the PA input and output, respectively, b_{CORR} and b_{SDC} are the optimum phase sequences using the CCOR and SDC measurement, respectively, and be calculated as follows

$$b_{CORR} = \arg_{b(i')} \max R_{xy}^{(0)} \quad 1 \le i' \le S \tag{24}$$

$$b_{SDC} = \arg_{b(i')} \max(SDC) \tag{25}$$

The proposed method has 2 stages. Firstly, selecting the S phase sequences which can produce the minimum PAPR amplitude among all the phase sequences, and finally selecting the optimum phase sequence which gives the highest similarity between the input and output signal of the amplifier among the selected phase sequences. The last stage is useful for BER reduction. Here is one tradeoff between the PAPR reduction and the BER reduction priority. By selecting S as a small value, this technique improves the PAPR

reduction performance and by selecting S as a large value improves the BER degradation performance.

3.4 Computational Complexity

The total complexity of the C-PTS [11] and the EPTS [13] techniques is given as:

$$C_{C-PTS} = 3VN/2 \log N + 2VW^{V-1}N \tag{26}$$

$$C_{EPTS} = 3/4VN\text{logN} + PVN \tag{27}$$

where N is the number of subcarriers, V is the number of subblocks and P is the number of iterations. The total complexity for the proposed method is expressed as:

$$C_{GCP} = 3/4VN\text{logN} + (P-1)VN/4 \tag{28}$$

$$C_{EGCP} = 3/4VN\text{logN} + (P-1)VN/12 \tag{29}$$

where C_{GCP} and C_{EGCP} are the total complexities of the *GCP* and *EGCP*, respectively. Equations 26 to 29 have 2 terms. The first term pertains to the complexity of the IFFT itself, and the second term is the complexity of the searching algorithm. Additionally, a complexity term is relevant to the similarity measurements that can be ignored due to its dependence on the value of parameter S. In other words, Eqs. 26–29 are defined for only one iteration, and the numbers of iterations in the first and second stages of the proposed method are not the same. This means that the number of iterations at the first stage is P, while the number of iterations at the second stage is S. Because of the small value of S, its non-effective complexity term can be omitted. Moreover, it should be highlighted that CCOR is less complex than SDC as the similarity measurement block [18], and this is an important difference, especially for implementation.

Table 1 presents the computational complexity of the CPTS and EPTS techniques and the proposed methods, GCP and EGCP, with $N = 512$ where CCRRGCP and CCRREGCP are the computational complexity reduction ratio (CCRR) [26] of the GCP and EGCP techniques over the EPTS respectively, whichis defined as:

$$CCRR = \left(1 - \frac{Complexity\ of\ the\ Proposed\ Method}{Complexity\ of\ the\ EPTS}\right) \times 100\% \tag{30}$$

For $V = 2$, the complexity of the CPTS technique is approximately the same as the EPTS technique when $D = 4$, the GCP when $D = 15$ and the EGCP when $D = 45$. The total

Table 1 Total Complexity of CPTS, EPTS, GCP and EGCP at V = 2 and V = 4 for different D values

Methods	V = 2						V = 4	
	D = 2	D = 4	D = 8	D = 15	D = 24	D = 45	D = 2	D = 4
CPTS	22016						289792	
EPTS	15104	23296	39680	68352	105216	191232	275968	538112
GCP	8704	10752	14848	22016	31232	52736	78848	144384
CCRRGCP%	42.3	53.84	62.58	67.79	70.31	72.42	71.42	73.16
EGCP	7500	8192	9550	11947	15019	22187	35499	57344
CCRREGCP%	50.28	64.83	75.91	82.52	85.72	88.39	87.13	89.34

complexity of the EPTS technique for $D = 2$ is approximately the same as the total complexity of the GCP and the EGCP for $D = 8$ and $D = 24$, respectively. The other comparison for $V = 4$ is shown, which proves that the complexity of the CPTS technique is approximately the same as the EPTS technique with $D = 2$, which is higher than the complexity of the proposed methods for $D = 4$. It should be noted that there is no need to calculate the complexity of the proposed method using the other D values because all the existing phase sequences could be covered by $D = 4$.

The only drawback of this method is the processing time due to the high iteration number, but *this high iteration number does not mean a high calculation in terms of the multiplication and addition operations*. Moreover, due to the *N/4* multiplier in each row, the computational delay time is 4 times less than that of the EPTS method. The resolution of this drawback is left to future work. Nevertheless, the simulation results based on the same iteration numbers show that the proposed method and the EPTS technique do not differ significantly in terms of PAPR reduction.

3.5 Side Information

To extract the original signal, side information is needed [32]. For the EPTS technique this is a $P \times N$ matrix. Therefore, a large matrix is needed to transmit by increasing the iteration numbers. This drawback is overcome in the proposed method because of the fixed phase sequence matrix. Therefore the number of optimum phase sequence row in the phase sequence matrix, acts as the side information which is needed to transmit, and there is no need to transmit phase sequence matrix.

3.6 Theoretical Proof

The theoretical proof is as following: In the CPTS and EPTS methods the phase sequences are selected randomly, when they should only be selected from (j, −j, 1, −1); therefore, there are only 4! (i.e., 24) different possible conditions, and each sample is forced to be multiplied by the same phases, frequently. Hence, there is a high probability of repetitive and redundant calculations, which is a drawback of the previous methods. In the GCP method, because of the phase sequence structure, and the assured difference between each row and its previous one, there is no redundant and repetitive calculations. On the other words, according to 4-ary Gray code and by analyzing the proposed matrix, each row has *N*/4 new phase sequences compared to the previous one. For example for $N = 256$, the 5th row has 64 and 128 different phases compared to the 4th and the 3rd rows, respectively. This decisive phase changes is so noteworthy to ensure the results. Furthermore, because of the arranged proposed matrix, all the samples are multiplied by the 24 possible conditions of the phases, definitely. Transferring the same calculations to the subsequent rows, and no need to do them repeatedly, is the framework of this method. Hence, by the decisive phase changes, the complexity term, PAPR performance, and the iteration number to achieve the desired PAPR value, is improved. Additionally, by using the similarity measurement block in the proposed structure, an improvement in terms of the BER performance is provided [18, 30].

4 Simulation Results

In this section, the PAPR performance and the BER reduction results are based on the computational complexity considerations and have been performed on *IEEE 802.16-based* networks. In the simulations, QPSK modulation with 10^6 random OFDM symbols is used. Figure 3 compares the CCDF of the CPTS, EPTS, GCP and EGCP techniques for $V = 2$, $W = 4$, $S = 10$, $L = 1$, and using the cross-correlation as the similarity measurement block. The simulation is based on a similar total complexity. Intuitively, the total complexity of all the techniques are approximately the same, which means that the complexity of the CPTS technique with $V = 2$ is about the same as the EPTS, GCP and EGCP techniques with $D = 4$, $D = 15$ and $D = 45$, respectively, as mentioned above. It can be observed that the proposed method is superior in terms of the PAPR performance compared to the CPTS and EPTS techniques by the same complexity due to the ability of more iteration use. Figure 4 illustrates the simulation of the PAPR performance of the mentioned techniques for $V = 4$, $W = 4$, $S = 10$ and $L = 1$. With $D = 4$, the proposed method can access all 256 iterations and achieve the maximum PAPR reduction results with a low total complexity compared to the CPTS technique. In addition, the effects of the different values of S on the PAPR reduction are simulated. It should be noted that the performance analysis in this section does not differ for $L = 1$ and $L = 4$ [13]; additionally, as mentioned above, the value of D and S should be considered by the user. The following are different values that can be used to evaluate the performance in different situations. Figure 5 compares the GCP technique by $V = 2$ and $D = 10$, for $S = 30$ and for $S = 100$. The results show that the small values for S outperform in terms of PAPR reduction.

The GCP and EPTS techniques are simulated with same iteration number, and the results are shown in Fig. 6. It is shown that by the same iteration number, the EPTS technique out-performs the GCP technique in terms of the PAPR reduction, but this difference is only slight and <0.5-dB at the PAPR above 8 dB. Figure 7 shows the BER performance of the GCP and CPTS techniques. The results are obtained using CCOR and

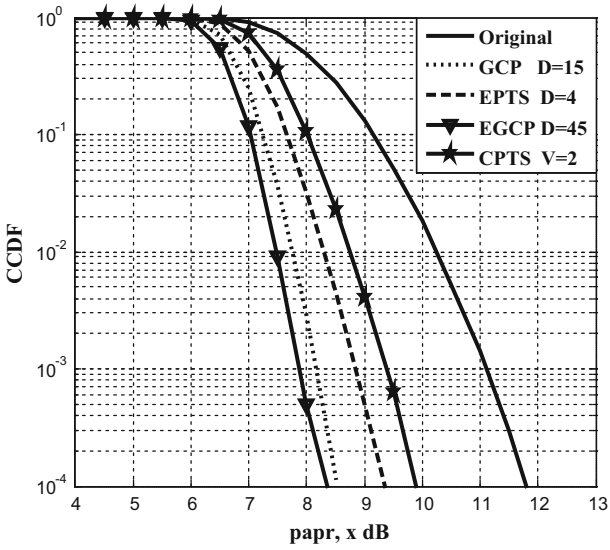

Fig. 3 CCDF of the GCP, EPTS, EGCP and CPTS techniques for V = 2, S = 10 and W = 4, for a comparison based on the same complexity

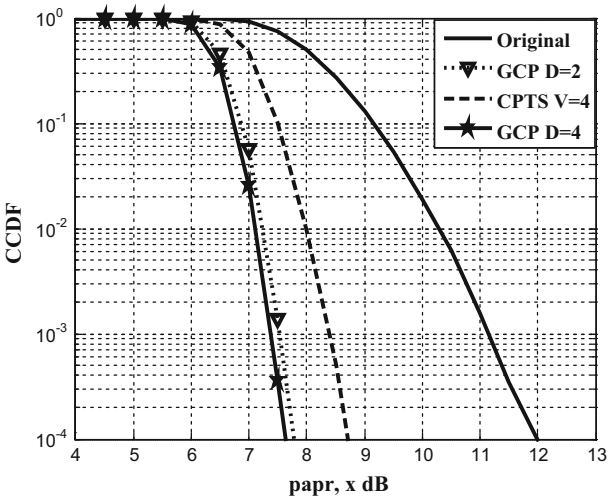

Fig. 4 CCDF of the GCP and CPTS techniques for V = 4, S = 10 and W = 4

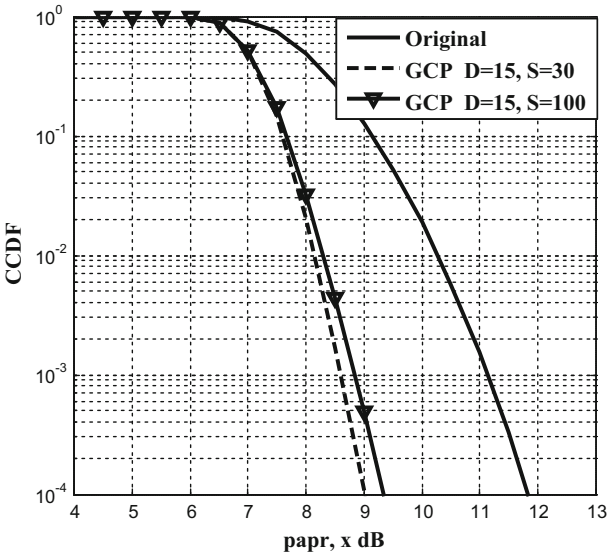

Fig. 5 A comparison of the GCP technique for different values of S, S = 30 and S = 100 when V = 2

SDC as the similarity measurement over the Rayleigh fading channel for $S = 30$ and $S = 100$ when $V = 2$.

The data symbols are selected from a 4-QAM symbol constellation. The Saleh model amplifier is used to represent the transmission of the power amplifier.

The results show that the GCP technique has a better BER performance compared to the CPTS. This performance is further improved with a high S value, so there is a better BER reduction performance for $S = 100$ compared to $S = 30$. It should be noted that both the CCOR and SDC similarity measurement blocks have the same results because of the same considered similarity percentage, which equals *90 % similarity*.

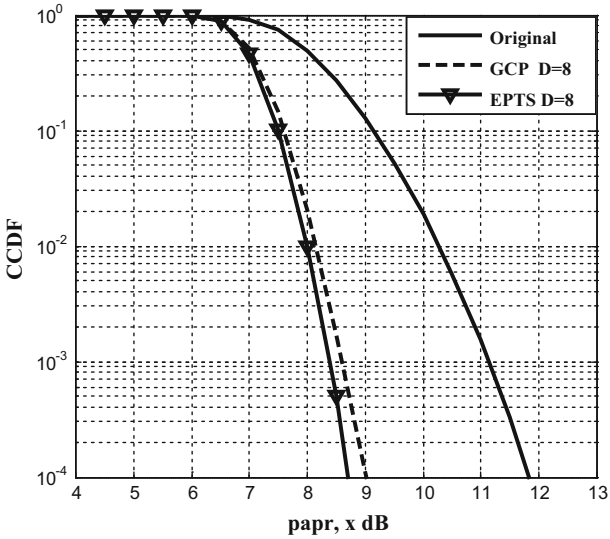

Fig. 6 Comparison of the GCP and EPTS techniques for the same iteration number, D = 8 when V = 2 and S = 10

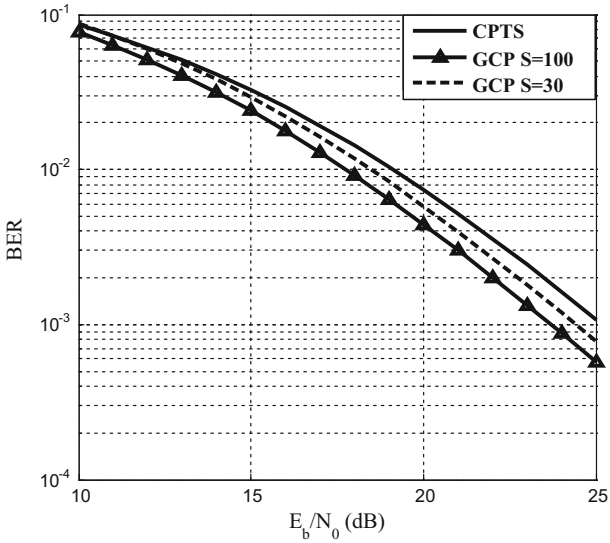

Fig. 7 BER of the CPTS and GCP techniques for S = 30 and S = 100 over the Rayleigh fading channel when V = 2

Thus, it is clear that the ability to increase the similarity percentage leads to a better BER performance.

Hence, a tradeoff between the PAPR reduction and the BER performance must be considered. Small *S* values present a better result in terms of PAPR reduction, while large *S* values give a better BER performance. All the figures except Fig. 3, discussed based on the GCP technique, not the EGCP. Because the performance results for the GCP and the EGCP techniques are the same and the difference is only on the complexity term as previously discussed.

5 Conclusion

This paper presents a low-complexity technique to reduce the PAPR and improve BER performance. This approach utilizes a matrix for a special structure of the Gray code. Firstly, all phase effects on the PAPR reduction have been examined, and then the *S* number of the minimum PAPR has been selected. Finally, the optimum phase sequence is the one with the highest similarity signal between the input and the output of the power amplifier among the *S* selected phase sequences. The complexity analysis shows that the proposed technique outperforms the CPTS and EPTS techniques in terms of PAPR reduction and BER performance while using approximately the same total complexity. The complexity analyses have demonstrated that with the same number of iterations, the total complexity is at least *42.3 %* less than that of the EPTS technique. Due to its low complexity, this technique can be applied in wireless communication systems to enhance the power efficiency and yield longer battery life.

Acknowledgments This work was supported by Universiti Putra Malaysia under the Prototype Development Research Grant Scheme (PRGS) No. 5528700.

References

1. Sakran, H., Shokair, M., El-Rabaie, E., & Nasr, O. (2013). Study the effect of PAPR on wideband cognitive OFDM radio networks. *Telecommunications Systems*. doi:10.1007/s11235-013-9708-z.
2. Varahram, P., Atlasbaf, Z., & Heydarian, N. (2005). Adaptive digital predistortion for power amplifiers used in CDMA applications. *In Proceedings of Asia-Pacific conference on applied electromagnetics, Malaysia* (pp. 215–218).
3. Mohammady, S., Varahram, P., Sidek, R. M., Hamidon, M. N., & Sulaiman, N. (2010). Efficiency improvement in microwave power amplifiers by using complex gain predistortion technique. *IEICE Electronics Express, 7*(23), 1721–1727.
4. Goff, S. Y. L., Khoo, B. K., Tsimenidis, C. C., & Sharif, B. S. (2008). A novel selected mapping technique for PAPR reduction in OFDM systems. *IEEE Transaction on Communications, 56*(11), 1775–1779.
5. Zhu, X., Jiang, T., & Zhu, G. (2008). Novel schemes based on greedy algorithm for PAPR reduction in OFDM systems. *IEEE Transaction on Consumer Electronic, 54*(3), 1048–1052.
6. Sabbaghian, M., Kwak, Y., Smida, B., & Tarokh, V. (2011). Nea Shannon limit and low peak to average power ratio turbo block coded OFDM. *IEEE Transactions on Communnications, 59*(8), 2042–2045.
7. Tsai, Y., Zhang, G., & Wang, X. (2008). Polyphase codes for uplink OFDM CDMA systems. *IEEE Transactions on Communications, 56*(6), 435–444.
8. Wang, X., Tjhung, T. T., & Ng, C. S. (1999). Reduction of peak-to-average power ratio of OFDM system using a companding technique. *IEEE Transactions on Broadcasting, 45*(3), 303–307.
9. Wang, Y., Wang, L. H., Ge, J. H., & Ai, B. (2012). Nonlinear companding transform technique for reducing PAPR of OFDM signals. *IEEE Transactions on Consumer Electronic, 58*(3), 752–757.
10. Ying Liang, H. (2015). Integrating CE and modified SLM to reduce the PAPR of OFDM systems. *Wireless Personal Communication*. doi:10.1007/s11277-014-2036-0.
11. Müller, S. H., Bäuml, R. W., Fischer, R. F. H., & Huber, J. B. (1997). OFDM with reduced peak-to-average power ratio by multiple signal representation. *Annales des Telecommunication, 52*(1–2), 58–67.
12. Baxley, R. J., & Zhou, G. T. (2007). Comparing selected mapping and partial transmit sequence for PAR reduction. *IEEE Transactions on Broadcasting, 53*(4), 797–803.
13. Varahram, P., & Ali, B. M. (2011). Partial transmit sequence scheme with phase sequence for PAPR reduction in OFDM systems. *IEEE Transactions on Consumer Electronic, 57*(2), 366–371.
14. Varahram, P., Mohammady, S., & Ali, B. M. (2013). A robust peak-to-average power ratio reduction scheme by inserting dummy signals with enhanced partial transmit sequence in OFDM systems. *Wireless Personal Communications, 72*(2), 1125–1137.
15. Mohammady, S., Sidek, R. M., Varahram, P., Hamidon, M. N., & Sulaiman, N. (2011). A new DSI-SLM method for PAPR reduction in OFDM systems. *IEEE international conference on consumer electronic, USA* (pp. 369–370).

16. Hu, S., Wu, G., Wen, Q., Xiao, Y., & Li, Sh. (2010). Nonlinearity reduction by tone reservation with null subcarriers for WiMAX system. *Wireless Personal Communication*. doi:10.1007/s11277-009-9726-z.
17. Krongold, B. S., & Jones, D. L. (2002). PAR reduction in OFDM via active constellation extension. *IEEE Transactions on Broadcasting, 49*(3), 258–268.
18. Al- Dalakta, E., Al- Dweik, A., Hazmi, A., & Tsimenidis, C. (2010). PAPR reduction scheme using maximum cross correlation. *IEEE Communication Letters, 16*(12), 2032–2035.
19. Nandalal, V., & Sophia, S. (2014). PAPR reduction of OFDM signal via custom conic optimized iterative adaptive clipping and filtering. *Wireless Personal Communication*. doi:10.1007/s11277-014-1788-x.
20. Zhu, X., Pan, W., Li, H., & Tang, Y. (2013). Simplified approach to optimized iterative clipping and filtering for PAPR reduction of OFDM signals. *IEEE Transactions on Communications, 61*(5), 1891–1901.
21. Taspinar, N., Kalinli, A., & Yildirim, M. (2011). Partial transmit sequences for PAPR reduction using parallel tabu search algorithm in OFDM systems. *IEEE Communication Letters, 15*(9), 974–976.
22. Wang, Y., Chen, W., & Tellambura, C. (2010). PAPR reduction method based on parametric minimum cross entropy for OFDM signals. *IEEE Communication Letters, 14*(6), 563–565.
23. Rodrigues, M. R. D., & Wassell, I. J. (2006). IMD reduction with SLM and PTS to improve the error-probability performance of nonlinearly distorted OFDM signals. *IEEE Transactions on Vehicular Technology, 55*(2), 537–548.
24. Sathananthan, K., & Tellambura, C. (2002). Partial transmit sequence and selected mapping schemes to reduce ICI in OFDM systems. *IEEE Communication Letters, 6*(8), 313–315.
25. Park, D., & Song, H. (2007). A new PAPR reduction technique of OFDM system with nonlinear high power amplifier. *IEEE Transactions on Consumer Electronic, 53*(2), 327–332.
26. Al-Dalakta, E., Al-Dweik, A., Hazmi, A., Tsimenidis, C., & Sharif, B. (2012). Efficient BER reduction technique for nonlinear OFDM transmission using distortion prediction. *IEEE Transactions on Vehicular Technology, 61*(5), 2330–2336.
27. Ahmed, S., & Kawai, M. (2013). Interleaving effects on BER fairness and PAPR in OFDMA system. *Telecommunication Systems*. doi:10.1007/s11235-011-9557-6.
28. Tellambura, C. (2001). Computation of the continuous-time PAR of an OFDM signal with BPSK subcarriers. *IEEE Communication Letters, 5*(5), 185–187.
29. Zhu, X., Jiang, T., & Zhu, G. (2008). Novel schemes based on greedy algorithm for PAPR reduction in OFDM systems. *IEEE Transactions on Consumer Electronic, 54*(3), 1048–1052.
30. Kazemian, M., Varahram, P., Hashim, S. J., Ali, M. B., Mohammady, S., & Sulaiman, N. (2014). Peak-to-average power ratio reduction based on cross-correlation in OFDM systems. *International conference on advanced communications technology*, *South Korea* (pp. 244–248).
31. Junjun, L., & Wei, Z. H. (2011). Low complexity PTS algorithm based on gray code and its FPGA implementation. *International conference on education and management innovation*, *China* (pp. 208–211).
32. Varahram, P., & Ali, B. M. (2011). A low complexity partial transmit sequence for peak to average power ratio reduction in OFDM systems. *Radio Engineering, 20*(3), 677–682.

Mohsen Kazemian received his B.Sc. electrical and electronics engineering in 2007, and his M.Sc. telecommunications engineering from Islamic Azad University in 2009. He is now Ph.D. student in University Putra Malaysia (UPM), on Wireless Telecommunication field. His research interest is PAPR reduction in OFDM wireless systems and Linearization of power amplifiers.

Pooria Varahram received his B.Sc. electrical and electronics engineering from khaje Nasir University of technology in 2002, his M.Sc. telecommunications engineering from tarbiat Modares University in 2004 and Ph.D. in wireless communication engineering from the University Putra Malaysia (UPM) in 2010. He has more than 8 years of experience in designing and developing a range of electronic and telecommunication related projects. He is now lecturer in Computer and Telecommunication Department in UPM. His research interest is PAPR reduction in OFDM systems, Linearization of power amplifiers, microwave power amplifiers design.

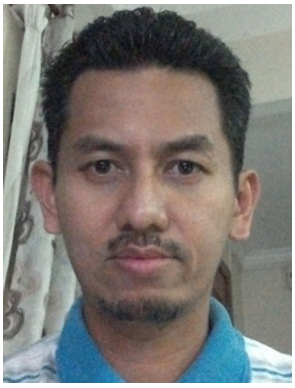

Shaiful Jahari Bin Hashim is currently a senior lecturer in the Department of Computer and Communication Systems Engineering, Faculty of Engineering, Universiti Putra Malaysia. He received his Ph.D. from Cardiff University, UK (2011), M.Sc from Universiti Kebangsaan Malaysia (2003) and B.Eng from University of Birmingham, UK (1998) in the field of Electrical and Electronics Engineering. His research interest is network security, cloud computing and wireless measurement system.

Borhanuddin Mohd Ali obtained his B.Sc. (Hons) Electrical and Electronics Engineering from Loughborough University in 1979; M.Sc. and Ph.D. from University of Wales, Cardiff, UK, in 1981 and 1985, respectively. He became a lecturer at UPM in 1985, and Professor in 2002 and served at various positions in UPM and various external organizations. He is a Senior Member of IEEE and a member of IET and a Chartered Engineer. He served at various positions in ComSoc and Malaysia Section, and IEEE Region 10, and presently Executive Co Chair of the ICC2016 Kuala Lumpur. His research interest spans Wireless Sensor Networks, Wireless Resource Management, Mobility, MIMO and OFDM, in which he published over 100 papers in refereed journals and over 200 conference papers.

Ronan Farrell received his BE and Ph.D. from University College Dublin in 1993 and 1998 respectively. In 2008 he became a strand co-leader for sensors networks in an SFI Cluster on advanced Geotechnologies with a focus on wide area wireless sensor networks. Ronan has published over a hundred peer-reviewed papers. He holds three patents and licensed technology that has led to the spin-out three companies, Ronan's personal research interests include wireless system design, electronics and radio systems.